A simple, highly visual *in vivo* screen for anaplastic lymphoma kinase inhibitors

Frederico S.L.M. Rodrigues[1,a,*], Xueyan Yang[1,b,*], Masataka Nikaido[1,c], Qingsong Liu[2] and Robert N. Kelsh[1#]

[1]*Centre for Regenerative Medicine and Department of Biology and Biochemistry, University of Bath, Claverton Down, Bath BA2 7AY, UK*

[2]*Dana Farber Cancer Institute, Harvard Medical School, Boston, MA and Department of Biological Chemistry and Molecular Pharmacology, Harvard Medical School, Boston, Massachusetts*

[*]These authors have contributed equally to this work and are to be considered joint first authors.

[a] Current affiliation: Division of Molecular Neurobiology, MRC National Institute for Medical Research, The Ridgeway, NW7 1AA London, United Kingdom.

[b] Current affiliation: MOE Key Laboratory of Contemporary Anthropology, School of Life Sciences, Fudan University, 220 Handan Rd., Shanghai, 200433, P.R. China.

[c] Current affiliation: Stowers Institute for Medical research, 1000E 50th street, Kansas City, MO, 64110, USA

[#]To whom correspondence should be addressed. E-mail: bssrnk@bath.ac.uk

Author contributions: F.S.L.M.R, X.Y., M.N., Q.L. and R.N.K. designed research; Q.L. contributed ALK inhibitors; F.S.L.M.R, X.Y. and M.N. performed research; F.S.L.M.R, X.Y., M.N. and R.N.K. analyzed data; and F.S.L.M.R, X.Y., M.N., Q.L.and R.N.K. wrote the paper.

The authors declare no conflict of interest.

Abstract

Anaplastic lymphoma kinase (ALK) is an important drug target in many cancers, including lymphoma, neuroblastoma and lung cancer. Here, we demonstrate proof-of-principle for a novel and inexpensive assay for ALK inhibitor activity and identification in zebrafish. We demonstrate that the human oncogenic ALK fusion, NPM-ALK, drives overproduction of iridophores, a highly visible, shiny pigment cell-type in zebrafish. Treatment with the potent ALK inhibitor, TAE684, fully inhibits production of ALK-dependent iridophores. Using our assay, we test multiple properties of TAE684 *in vivo*, including efficacy, specificity and toxicity. We note that TAE684 also inhibits the closely-related leukocyte tyrosine kinase (Ltk) that is required for endogenous iridophore development. Similar effects are observed with an independent inhibitor, Crizotinib. Our assay can thus be utilised to identify ALK or LTK inhibitors. Importantly, the natural reflectivity of iridophores lends itself to automation for high throughput assessment of ALK and LTK inhibitor compounds *in vivo*.

Introduction

Receptor tyrosine kinases (RTKs) are a large family of transmembrane receptor proteins with widespread functions in embryonic development (*1*). They usually function by ligand-induced dimerization, resulting in trans-phosphorylation of the intracellular kinase domain, and generating docking sites for various adaptor proteins triggering multiple intracellular signalling cascades. Elevated RTK activity is a common cause of human disease, so that effective RTK inhibitor compounds are in great demand as therapeutic agents (*2*).

Anaplastic lymphoma kinase (ALK) is an RTK, first identified in human anaplastic large cell lymphoma (ALCL (*3*)), but subsequently shown to be a key driver in a subset of cancers, including neuroblastoma, non-small cell lung cancer (NSCLC), and inflammatory myofibroblastic tumours (IMT) (*4-8*). In all cases, disease is associated with elevated ALK signalling, due either to gene amplification or activating mutations. In neuroblastoma, activating point mutations (e.g. F1174L) are most common (*5, 7, 9, 10*). In ALCL, IMT and NSCLC, constitutive kinase signalling usually results from translocation events generating abnormal fusion proteins (*11*), such as the frequent t(2,5)(p23;q35) translocation resulting in expression of a nucleophosmin (NPM)-ALK fusion protein (*3*).

Validation of ALK as an important therapeutic target has led to the development of ALK inhibitors, including both the clinically-approved drug Crizotinib (PF-2341066) [**1**] and TAE684 [**2**](**Figure 1**), shown to be effective in various *in vitro* and *in vivo* preclinical and clinical models (*12, 13,14, 15*). However, Crizotinib resistance is already being seen clinically, in one patient resulting from the acquisition of the F1174L mutation in the kinase domain (*15*), underlining the need for novel assays to develop ALK inhibitors working through different modalities.

Zebrafish have become a valuable research platform for drug discovery and development because of the ease of detection of drug efficacy in intact embryos.

Previously, we have shown that loss-of-function alleles for leukocyte tyrosine kinase (Ltk), the sister kinase to ALK, lack iridophores in zebrafish (*16*). Iridophores are neural crest-derived pigment cells that are clearly visible as shiny silver cells in the developing zebrafish embryo. Zebrafish *ltk* is expressed in the neural crest cells, and acts cell-autonomously to drive fate-specification of iridophores; *ltk* mutants lack iridophores due to a failure of this iridophore fate specification process, but show otherwise normal body morphology (*16*). Noting the structural similarity between the LTK and ALK kinase domains, we reasoned that constitutively activated ALK variants might be able to substitute for Ltk function if they were expressed in the zebrafish neural crest. If so, we then would be able to test the functional activity of human ALK cancer mutations as well as their sensitivity to small molecule inhibition in the zebrafish system by using iridophore numbers as a straight-forward phenotypic read-out of ALK activity. Here we report that expression of the human oncogenic ALK fusion, NPM-ALK, in zebrafish neural crest restores iridophore development in *ltk* mutant embryos, and can also promote ectopic and supernumerary iridophores in wild-type embryos. In addition, we used the small molecule ALK inhibitor, TAE684 (*13*), to provide proof-of-principle evidence that loss of NPM-ALK-dependent iridophores can be used as a simple, *in vivo* assay for ALK inhibition. We also observed TAE684-dependent phenocopying of the *ltk* mutant phenotype, and show that this compound also shows inhibitory activity against Ltk, consistent with kinome-wide selectivity profiling data. Furthermore, at higher doses of TAE684 non-specific effects including shortened body axis and embryonic lethality become apparent. Likewise, we show that Crizotinib treatment also inhibits ALK-dependent iridophores in our zebrafish assay. Treatment with a MEK inhibitor also decreased iridophore numbers and sensitized the response to Crizotinib, suggesting that MEK signaling lies downstream of ALK/Ltk signaling in iridophore specification. Our studies identify powerful new *in vivo* assays for ALK and LTK inhibitor screening.

Results and Discussion

Human NPM-ALK expression can rescue loss of Ltk signaling in zebrafish. In zebrafish, iridophores are prominent shiny cells that cover the eyes, and form a series of spots above the brain and above and below the trunk and tail segmental muscle blocks (**Figure 2b**). We have shown that *ltk* mutants form an allelic series, with the strongest alleles (e.g. *ltk*^{ty82}; **Figure 2d, h**) resulting in embryos showing no iridophores, whereas mutants for intermediate alleles have only reduced iridophore numbers; in all other respects embryos are morphologically normal, except that the swim bladder fails to inflate (*16*). Similarly, morpholino knockdown of Ltk in wild-type embryos gave good phenocopies of the *ltk* mutant phenotypes (*16*). In *ltk*^{ty82} mutants (hereafter referred to as *ltk* mutants) a premature stop codon results in a predicted protein that is truncated and completely lacks the tyrosine kinase domain. ALK is 64% identical at the amino acid level to LTK (*17*). We tested whether the human oncogenic ALK variant, NPM-ALK, which has constitutively active kinase signaling (*18, 19*), would rescue the *ltk* phenotype (**Figure 2a**). We generated an expression construct, p*sox10:NPM-ALK*, encoding the NPM-ALK fusion under the control of the *sox10* promoter shown to drive expression in neural crest (*20*). Injection of this construct into 1-cell stage *ltk* mutants resulted in prominent rescue of iridophores compared with uninjected siblings (**Figure 2d,e**). At the doses used in these initial studies, we also saw substantial early embryonic lethality, but nevertheless rescue was observed in c. 25% of surviving mutant embryos, consistent with the expected highly mosaic distribution of the injected plasmid DNA and with the strictly localized expression of the *sox10* promoter. Rescued iridophores tend to form striking clusters in a position dorsal to the neural tube (**Figure 2e**). Furthermore, injected wild-type sibling embryos often showed supernumerary and/or ectopic iridophores in addition to the normal complement of (*ltk*-dependent) iridophores (**Figure 2b,c**).

We also tested an analogous construct, p*sox10:NPM-Ltk*, in which the ALK coding region from the NPM-ALK construct was substituted with the equivalent region of

zebrafish Ltk. Again, injection of this construct rescued iridophore development in a proportion of *ltk* mutant embryos, and generated supernumerary and/or ectopic cells in wild-type siblings (**Figure 2f-i**). We note that we have previously used the same plasmid, but with GFP or Cre in place of NPM-ALK or NPM-Ltk, to make transgenic lines, none of which show changed iridophore patterns (*20, 21*); similarly a kinase-dead version of the NPM-Ltk construct fails to generate supernumerary/ectopic iridophores (MN and RNK, unpub. data). We conclude that both the human oncogenic NPM-ALK and the NPM-Ltk proteins are able to drive neural crest cells to form iridophores, and can substitute for endogenous Ltk activity.

ALK inhibitor treatment inhibits NPM-ALK activity *in vivo*. These results immediately suggested that the efficacy of candidate ALK inhibitors might be assessed *in vivo* by their addition to the bathing media of transient transgenic NPM-ALK embryos; effective compounds should inhibit both the NPM-ALK-dependent iridophores in *ltk* mutants and the NPM-ALK-dependent supernumerary/ectopic cells in wild-type embryos. To test this idea, we asked whether the new ALK inhibitor TAE684, known to be active against the NPM-ALK fusion in a mammalian context (*13*), inhibited the effects of NPM-ALK expression in the zebrafish. We injected wild-type embryos with p*sox10:NPM-ALK*, while control embryos were left uninjected. A lower dose of DNA was used in these experiments compared with those described before; this had the advantage of lowered embryonic mortality, whilst still retaining a readily detectable iridophore phenotype. A proportion of each set of embryos was treated with 2 µM TAE684, whereas the remainder were treated with 1% DMSO alone (**Figure 3a**). At 3 days post fertilisation (dpf) the iridophore pattern of each embryo was assigned to one of three categories: i) *normal* iridophore pattern, a series of spots above dorsal neural tube, but lacking at this stage in dorsal head; ii) embryos with *supernumerary* or *ectopic* iridophores; and iii) embryos with *decreased* numbers of iridophores (**Figure 3**). Injection of p*sox10:NPM-ALK* into wild-type embryos gave the expected

supernumerary/ectopic iridophore phenotype, whereas plasmid injected, TAE684-treated sibling embryos showed a striking reduction in this phenotype (**Figure 3c,d**; quantitated in **e**). We conclude that treatment of transient transgenic embryos with TAE684 provides effective inhibition of NPM-ALK-dependent iridophore development, providing proof-of-principle that our assay can be used to identify *in vivo* efficacy of ALK inhibitors.

To confirm this phenotype reflected a specific effect of ALK inhibition, rather than a coincidental off-target activity that also affects iridophores, we assessed the effects of Crizotinib in our assay. Crizotinib is an ALK/c-MET dual inhibitor with distinct pharmacophore and selectivity profile to TAE684. It has recently been demonstrated to be the most selective for ALK of a set of 72 kinase inhibitors profiled on >440 kinases in a competitive binding assay (*22*). We repeated our test for inhibition of NPM-ALK expressing embryos using Crizotinib treatment and see that this treatment also reduces the number of embryos showing ectopic or supernumerary iridophores (**Figure 3f**). We then tested whether this effect can be enhanced by treatment with a sub-optimal dose of a MEK inhibitor, PD0325901 [**3**] (**Figure 1**), on the basis that MEK signalling is a major pathway downstream of receptor tyrosine kinase signalling (*23*). Interestingly, a 500 nM dose of PD0325901 alone did not cause a pronounced inhibition of NPM-ALK-dependent iridophores (**Figure 3f**). In contrast, combined treatment of NPM-ALK injected fish with both PD0325901 and Crizotinib gives an enhanced inhibition of the ectopic/supernumerary cells (**Figure 3f**). We conclude that two independent ALK inhibitors each inhibit the iridophore-inducing effect of NPM-ALK expression in zebrafish, strongly supporting the suggestion that ALK activity is the key factor driving these cells. In addition, our screen appears to be sensitised by treatment with low doses of MEK inhibitor.

TAE684 and Crizotinib-treatment inhibit Ltk activity in zebrafish. Given the sister kinase relationship of ALK and LTK, it is expected that even selective ALK inhibitors

might also show activity against LTK. Crizotinib showed strong inhibition of c-Met and ALK out of a panel of 120 kinases, although it is not clear whether these included LTK (*24*). In a cell proliferation assay TAE684 proved highly selective, being at least 100-fold more effective against ALK than against 20 other kinases tested (*13*), although the kinase panel tested did not include LTK. Specificity was higher in cellular assays than in direct enzymatic assays, and modelling suggested that part, but not all, of the specificity depended upon the bulk of the amino acid residue at position 258; we note that ALK and LTK in both human and zebrafish all have a conserved eu258 residue (**Supp. Figure 1**). Biochemical profiling of both TAE684 and Crizotinib showed very similar strength of competitive binding of these compounds to both ALK and LTK as measured by Ambit Bioscience KinomeScan^{TM} profiling, although the interaction profiles with other kinases in the panels tested were generally distinct (*22, 25*)(N. Gray, pers. comm.). In addition, TAE684 shows a 50% inhibitory concentration (IC50) of 18 nM against LTK using Life Technologies Corporation, SelectScreen$^{®}$ Kinase Profiling. Taken together, we considered that activity of TAE684 and Crizotinib against the zebrafish Ltk, in addition to ALK, *in vivo* was likely. Ltk loss-of-function mutants show graded degrees of iridophore number decrease (*16, 26*). In our treatment of wild-type embryos with TAE684 we noticed that embryos frequently phenocopied *ltk* mutant embryos (**Figure 3e**). Likewise, embryos treated with TAE684 and the NPM-ALK plasmid rarely showed the clean loss of the NPM-ALK-dependent iridophores alone, but instead usually showed a dramatic decrease in all iridophores (**Figure 3d,e**). Interestingly, the degree of iridophore decrease was dose-dependent (**Supp. Figure 2a-d'**), clearly phenocopying the allelic series of *ltk* mutant alleles (*16*). Similar observations were made with Crizotinib-treated embryos (**Supp. Figure 2e**; data not shown). Again, we saw sensitisation of this screen by low-dose treatment with the MEK inhibitor PD0325901 (**Supp. Figure 2e**). We hypothesised that, in addition to inhibition of the NPM-ALK protein, both Crizotinib and TAE684 were also inhibiting endogenous Ltk activity.

To test more directly whether TAE684 might inhibit Ltk kinase activity in our *in vivo* context, we asked whether TAE684-treatment prevented the supernumerary/ectopic iridophores induced by injection of p*sox10:NPM-Ltk*. As predicted, we saw that TAE684 inhibited formation of ectopic iridophores, and that this effect was often combined with loss of the endogenous cells (**Figure 4**). We conclude that TAE684 shows significant *in vivo* activity as an Ltk inhibitor, and that this is highly likely for Crizotinib too.

Specificity of RTK inhibitor phenotypes *in vivo*. While both TAE684 and Crizotinib show specific inhibition of exogenous ALK and endogenous and exogenous Ltk, the *in vivo* phenotypes are consistent with them not affecting other RTKs. For example, we never observed effects on other neural crest-derived pigment cells, including melanocytes, in TAE684 or Crizotinib-treated embryos. This is notable since mutations in the RTK Kit result in a prominent decrease in melanocyte numbers, a phenotype that is phenocopied by treatment of embryos with PDGFR/Kit tyrosine kinase inhibitor IV [**5**] (**Figure 1**; **Supp. Figure 3a-a''**; (*26, 27*). Thus, *in vivo*, TAE684 and Crizotinib appear to show no activity at these doses against Kit, consistent with the findings in cell proliferation studies (*13*).

Conversely, we do not generally observe strong iridophore phenotypes with inhibitors directed against other RTKs. For example, treatment of wild-type embryos with the PDGFR/Kit inhibitor did not affect iridophores at doses that phenocopied the Kit mutant phenotype (data not shown). At higher doses, there were additional severe defects in eye and body morphology, consistent with off-target effects (**Supp. Figure 3a', a''**). Our results with the VEGFR inhibitor, Vatalanib (also known as PTK787/ZK222584) [**4**](**Figure 1**), were particularly interesting. Inhibition of VEGF-R using Vatalanib results in defective growth of blood vessels (*28*). We were able to reproduce these findings using doses of even just 1.25 uM, but did not see consistent reduction in iridophores at

this dose (**Supp. Figure 3b**). This inhibitor is reported to show some activity against ALK (*29*), and thus may also be expected to target LTK too, which likely explains why we do see an effect on iridophore numbers at higher doses (**Supp. Figure 3b**).

In our dose-response experiment (**Supp. Figure 2**) we observed shortening of the body axis at 6 µM, and embryonic lethality at 10 µM, suggesting that higher doses induced substantial off-target effects. Nevertheless, the specific inhibition of iridophore phenotypes occurred cleanly at lower doses. We conclude that our iridophore assay is specific to ALK and Ltk activity, and effects of drug treatment on other targets often result in detectable, but distinct, phenotypes.

Conclusion

We have developed the zebrafish system as a simple and effective assay for ALK inhibition *in vivo*. We use iridophore number as a direct functional readout of oncogenic ALK activity, allowing a simple visual screen for chemical inhibitors of that activity. We show that inhibition of oncogenic ALK can be distinguished from effects on even the very closely-related Ltk (comparing supernumerary versus endogenous iridophore numbers).

We also show that Ltk iridophore activity is sensitive to TAE684 (and likely Crizotinib), providing a parallel assay to assess Ltk activity based on screening wild-type embryos for reduction of iridophores. Such a screen may be useful in the identification of drug-leads against LTK, which may have application in treatment of systemic lupus erythematosis (*30*). Such a screen might also identify additional ALK inhibitors, however the ALK inhibitor assay described here has the advantages of directly assessing inhibition of the *human oncogenic* protein and of being straight-forward to adapt to other oncogenic ALK variants, including activating point mutations such as are found in Inflammatory myoblastic tumour and neuroblastoma (*9, 10, 15*). We note also that our data indicates that use of low doses of MEK inhibitor PD0325901

provides a sensitised ALK inhibitor screen which may be advantageous when searching for novel lead compounds.

One limitation of the current assay is the mosaicism due to the transient transgenic nature of the embryos used. Further refinement of our assay using conditionally-expressing transgenic lines (*31*) to allow us to ensure that all embryos express the transgene in all neural crest cells without constitutive lethality would substantially improve assay efficiency, and would facilitate the screening of large numbers of molecules. Iridophores are auto-fluorescent and combined with recent advances in high-throughput microscopy (*32*), our assay can be readily adapted to an automated, quantitative assessment of *in vivo* ALK kinase activity. Zebrafish are increasingly popular for medium-large scale drug screens, where the embryos' small size, optical clarity, external development in aqueous medium, and ease of genetic manipulation to make transgenic reporter lines, make them ideally suited (*33, 34*).

In summary, we believe that our assay is unique in combining several powerful features in an *in vivo* context including: 1) quantitative readout of functional activity of ALK mutations; 2) sensitive detection of off-target effects; 3) potential for automation for high-throughput; 4) suitability for screening for genetic and chemical suppressor mutations, and for 5) testing combination therapies on resistant ALK mutations. Given the significant animal welfare and cost advantages of using zebrafish embryos, our assay system offers substantial opportunities for early assessment of *in vivo* efficacy and specificity of lead molecules in the drug development pipeline. These assays might even be further adapted for other RTKs, thus offering even greater utility as a drug development tool.

Methods

Full details of methods used are provided in the supplementary material that accompanies this paper online.

Figure

Acknowledgements

We wish to thank S. Elworthy for the original suggestion to use the NPM-ALK assay as a kinase inhibitor screen, R. Jäger for the NPM-ALK clone and C Chien for IRES-eGFP fragment, N. Gray, P. Jänne, and C. Miduturu for providing kinase profiling data. We thank C. de Paiva for technical assistance with some Vatalanib experiments. We are grateful to C. Anastasaki for the schematic figures and to M. Morais for the chemical structure figures. We thank E. Patton for comments on versions of this manuscript. We gratefully acknowledge the support of the MRC (grant G0400806, RNK), the Wellcome Trust (grants 066326 and 077454) and Fundação para a Ciência e Tecnologia (FCT; FSLMR) for funding this work.

Supporting information available: Full materials and methods and supplementary figures. This material is available free of charge via the Internet at http://pubs.acs.org.

References

1. Lemmon, M. A., and Schlessinger, J. (2010) Cell signaling by receptor tyrosine kinases, *Cell 141*, 1117-1134.
2. Zhang, J., Yang, P. L., and Gray, N. S. (2009) Targeting cancer with small molecule kinase inhibitors, *Nat Rev Cancer 9*, 28-39.
3. Morris, S. W., Kirstein, M. N., Valentine, M. B., Dittmer, K. G., Shapiro, D. N., Saltman, D. L., and Look, A. T. (1994) Fusion of a kinase gene, ALK, to a nucleolar protein gene, NPM, in non-Hodgkin's lymphoma, *Science 263*, 1281-1284.
4. Caren, H., Abel, F., Kogner, P., and Martinsson, T. (2008) High incidence of DNA mutations and gene amplifications of the ALK gene in advanced sporadic neuroblastoma tumours, *Biochem J 416*, 153-159.
5. Janoueix-Lerosey, I., Lequin, D., Brugieres, L., Ribeiro, A., de Pontual, L., Combaret, V., Raynal, V., Puisieux, A., Schleiermacher, G., Pierron, G., Valteau-Couanet, D., Frebourg, T., Michon, J., Lyonnet, S., Amiel, J., and Delattre, O. (2008) Somatic and germline activating mutations of the ALK kinase receptor in neuroblastoma, *Nature 455*, 967-970.
6. Lawrence, B., Perez-Atayde, A., Hibbard, M. K., Rubin, B. P., Dal Cin, P., Pinkus, J. L., Pinkus, G. S., Xiao, S., Yi, E. S., Fletcher, C. D., and Fletcher, J. A. (2000) TPM3-ALK and TPM4-ALK oncogenes in inflammatory myofibroblastic tumors, *Am J Pathol 157*, 377-384.
7. Mosse, Y. P., Laudenslager, M., Longo, L., Cole, K. A., Wood, A., Attiyeh, E. F., Laquaglia, M. J., Sennett, R., Lynch, J. E., Perri, P., Laureys, G., Speleman, F., Kim, C., Hou, C., Hakonarson, H., Torkamani, A., Schork, N. J., Brodeur, G. M., Tonini, G. P.,

Rappaport, E., Devoto, M., and Maris, J. M. (2008) Identification of ALK as a major familial neuroblastoma predisposition gene, *Nature 455*, 930-935.

8. Soda, M., Choi, Y. L., Enomoto, M., Takada, S., Yamashita, Y., Ishikawa, S., Fujiwara, S., Watanabe, H., Kurashina, K., Hatanaka, H., Bando, M., Ohno, S., Ishikawa, Y., Aburatani, H., Niki, T., Sohara, Y., Sugiyama, Y., and Mano, H. (2007) Identification of the transforming EML4-ALK fusion gene in non-small-cell lung cancer, *Nature 448*, 561-566.
9. George, R. E., Sanda, T., Hanna, M., Frohling, S., Luther, W., 2nd, Zhang, J., Ahn, Y., Zhou, W., London, W. B., McGrady, P., Xue, L., Zozulya, S., Gregor, V. E., Webb, T. R., Gray, N. S., Gilliland, D. G., Diller, L., Greulich, H., Morris, S. W., Meyerson, M., and Look, A. T. (2008) Activating mutations in ALK provide a therapeutic target in neuroblastoma, *Nature 455*, 975-978.
10. Chen, Y., Takita, J., Choi, Y. L., Kato, M., Ohira, M., Sanada, M., Wang, L., Soda, M., Kikuchi, A., Igarashi, T., Nakagawara, A., Hayashi, Y., Mano, H., and Ogawa, S. (2008) Oncogenic mutations of ALK kinase in neuroblastoma, *Nature 455*, 971-974.
11. Mosse, Y. P., Wood, A., and Maris, J. M. (2009) Inhibition of ALK signaling for cancer therapy, *Clin Cancer Res 15*, 5609-5614.
12. Christensen, J. G., Zou, H. Y., Arango, M. E., Li, Q., Lee, J. H., McDonnell, S. R., Yamazaki, S., Alton, G. R., Mroczkowski, B., and Los, G. (2007) Cytoreductive antitumor activity of PF-2341066, a novel inhibitor of anaplastic lymphoma kinase and c-Met, in experimental models of anaplastic large-cell lymphoma, *Mol Cancer Ther 6*, 3314-3322.
13. Galkin, A. V., Melnick, J. S., Kim, S., Hood, T. L., Li, N., Li, L., Xia, G., Steensma, R., Chopiuk, G., Jiang, J., Wan, Y., Ding, P., Liu, Y., Sun, F., Schultz, P. G., Gray, N. S., and Warmuth, M. (2007) Identification of NVP-TAE684, a potent, selective, and efficacious inhibitor of NPM-ALK, *Proc. Natl. Acad. Sci. U. S. A. 104*, 270-275.
14. Kwak, E. L., Bang, Y. J., Camidge, D. R., Shaw, A. T., Solomon, B., Maki, R. G., Ou, S. H., Dezube, B. J., Janne, P. A., Costa, D. B., Varella-Garcia, M., Kim, W. H., Lynch, T. J., Fidias, P., Stubbs, H., Engelman, J. A., Sequist, L. V., Tan, W., Gandhi, L., Mino-Kenudson, M., Wei, G. C., Shreeve, S. M., Ratain, M. J., Settleman, J., Christensen, J. G., Haber, D. A., Wilner, K., Salgia, R., Shapiro, G. I., Clark, J. W., and Iafrate, A. J. (2010) Anaplastic lymphoma kinase inhibition in non-small-cell lung cancer, *N Engl J Med 363*, 1693-1703.
15. Sasaki, T., Okuda, K., Zheng, W., Butrynski, J., Capelletti, M., Wang, L., Gray, N. S., Wilner, K., Christensen, J. G., Demetri, G., Shapiro, G. I., Rodig, S. J., Eck, M. J., and Janne, P. A. (2010) The neuroblastoma associated F1174L ALK mutation causes resistance to an ALK kinase inhibitor in ALK translocated cancers, *Cancer Res 70*, 10038-10043.
16. Lopes, S. S., Yang, X., Muller, J., Carney, T. J., McAdow, A. R., Rauch, G. J., Jacoby, A. S., Hurst, L. D., Delfino-Machin, M., Haffter, P., Geisler, R., Johnson, S. L., Ward, A., and Kelsh, R. N. (2008) Leukocyte tyrosine kinase functions in pigment cell development, *PLoS Genet 4*, e1000026.
17. Morris, S. W., Naeve, C., Mathew, P., James, P. L., Kirstein, M. N., Cui, X., and Witte, D. P. (1997) ALK, the chromosome 2 gene locus altered by the t(2;5) in non-Hodgkin's lymphoma, encodes a novel neural receptor tyrosine kinase that is highly related to leukocyte tyrosine kinase (LTK), *Oncogene 14*, 2175-2188.
18. Bai, R. Y., Dieter, P., Peschel, C., Morris, S. W., and Duyster, J. (1998) Nucleophosmin-anaplastic lymphoma kinase of large-cell anaplastic lymphoma is a constitutively active tyrosine kinase that utilizes phospholipase C-gamma to mediate its mitogenicity, *Mol. Cell Biol. 18*, 6951-6961.

19. Shiota, M., Fujimoto, J., Semba, T., Satoh, H., Yamamoto, T., and Mori, S. (1994) Hyperphosphorylation of a novel 80 kDa protein-tyrosine kinase similar to Ltk in a human Ki-1 lymphoma cell line, AMS3, *Oncogene 9*, 1567-1574.
20. Dutton, J. R., Antonellis, A., Carney, T. J., Rodrigues, F. S., Pavan, W. J., Ward, A., and Kelsh, R. N. (2008) An evolutionarily conserved intronic region controls the spatiotemporal expression of the transcription factor Sox10, *BMC Dev Biol 8*, 105.
21. Rodrigues, F. S., Doughton, G., Yang, B., and Kelsh, R. N. (2012) A novel transgenic line using the Cre-lox system to allow permanent lineage-labeling of the zebrafish neural crest, *Genesis*.
22. Davis, M. I., Hunt, J. P., Herrgard, S., Ciceri, P., Wodicka, L. M., Pallares, G., Hocker, M., Treiber, D. K., and Zarrinkar, P. P. (2011) Comprehensive analysis of kinase inhibitor selectivity, *Nat Biotechnol 29*, 1046-1051.
23. Chiarle, R., Voena, C., Ambrogio, C., Piva, R., and Inghirami, G. (2008) The anaplastic lymphoma kinase in the pathogenesis of cancer, *Nat Rev Cancer 8*, 11-23.
24. Zou, H. Y., Li, Q., Lee, J. H., Arango, M. E., McDonnell, S. R., Yamazaki, S., Koudriakova, T. B., Alton, G., Cui, J. J., Kung, P. P., Nambu, M. D., Los, G., Bender, S. L., Mroczkowski, B., and Christensen, J. G. (2007) An orally available small-molecule inhibitor of c-Met, PF-2341066, exhibits cytoreductive antitumor efficacy through antiproliferative and antiangiogenic mechanisms, *Cancer Res 67*, 4408-4417.
25. Hellwig, S., Miduturu, C. V., Kanda, S., Zhang, J., Filippakopoulos, P., Salah, E., Deng, X., Choi, H. G., Zhou, W., Hur, W., Knapp, S., Gray, N. S., and Smithgall, T. E. (2012) Small-Molecule Inhibitors of the c-Fes Protein-Tyrosine Kinase, *Chem Biol 19*, 529-540.
26. Parichy, D. M., Rawls, J. F., Pratt, S. J., Whitfield, T. T., and Johnson, S. L. (1999) Zebrafish sparse corresponds to an orthologue of c-kit and is required for the morphogenesis of a subpopulation of melanocytes, but is not essential for hematopoiesis or primordial germ cell development, *Development 126*, 3425-3436.
27. Colanesi, S., Taylor, K. L., Temperley, N. D., Lundegaard, P. R., Liu, D., North, T. E., Ishizaki, H., Kelsh, R. N., and Patton, E. E. (2012) Small molecule screening identifies targetable zebrafish pigmentation pathways, *Pigment Cell Melanoma Res 25*, 131-143.
28. Chan, J., Bayliss, P. E., Wood, J. M., and Roberts, T. M. (2002) Dissection of angiogenic signaling in zebrafish using a chemical genetic approach, *Cancer Cell 1*, 257-267.
29. Hess-Stumpp, H., Haberey, M., and Thierauch, K. H. (2005) PTK 787/ZK 222584, a tyrosine kinase inhibitor of all known VEGF receptors, represses tumor growth with high efficacy, *Chembiochem 6*, 550-557.
30. Li, N., Nakamura, K., Jiang, Y., Tsurui, H., Matsuoka, S., Abe, M., Ohtsuji, M., Nishimura, H., Kato, K., Kawai, T., Atsumi, T., Koike, T., Shirai, T., Ueno, H., and Hirose, S. (2004) Gain-of-function polymorphism in mouse and human Ltk: implications for the pathogenesis of systemic lupus erythematosus, *Hum Mol Genet 13*, 171-179.
31. Langenau, D. M., Feng, H., Berghmans, S., Kanki, J. P., Kutok, J. L., and Look, A. T. (2005) Cre/lox-regulated transgenic zebrafish model with conditional myc-induced T cell acute lymphoblastic leukemia, *Proc. Natl. Acad. Sci. U. S. A. 102*, 6068-6073.
32. Pardo-Martin, C., Chang, T. Y., Koo, B. K., Gilleland, C. L., Wasserman, S. C., and Yanik, M. F. (2010) High-throughput in vivo vertebrate screening, *Nat Methods 7*, 634-636.
33. Zon, L. I., and Peterson, R. T. (2005) In vivo drug discovery in the zebrafish, *Nat Rev Drug Discov 4*, 35-44.
34. Kokel, D., Bryan, J., Laggner, C., White, R., Cheung, C. Y., Mateus, R., Healey, D., Kim, S., Werdich, A. A., Haggarty, S. J., Macrae, C. A., Shoichet, B., and Peterson, R. T. (2010) Rapid behavior-based identification of neuroactive small molecules in the zebrafish, *Nat Chem Biol 6*, 231-237.
35. Kimmel, C. B., Ballard, W. W., Kimmel, S. R., Ullmann, B., and Schilling, T. F. (1995) Stages of Embryonic Development of the Zebrafish, *Dev. Dynamics 203*, 253-310.

36. Notredame, C., Higgins, D. G., and Heringa, J. (2000) T-Coffee: A novel method for fast and accurate multiple sequence alignment, *J. Mol. Biol. 302*, 205-217.
37. Armougom, F., Moretti, S., Poirot, O., Audic, S., Dumas, P., Schaeli, B., Keduas, V., and Notredame, C. (2006) Expresso: automatic incorporation of structural information in multiple sequence alignments using 3D-Coffee, *Nucleic Acids Res 34*, W604-608.
38. Barrett, S. D., Bridges, A. J., Dudley, D. T., Saltiel, A. R., Fergus, J. H., Flamme, C. M., Delaney, A. M., Kaufman, M., LePage, S., Leopold, W. R., Przybranowski, S. A., Sebolt-Leopold, J., Van Becelaere, K., Doherty, A. M., Kennedy, R. M., Marston, D., Howard, W. A., Jr., Smith, Y., Warmus, J. S., and Tecle, H. (2008) The discovery of the benzhydroxamate MEK inhibitors CI-1040 and PD 0325901, *Bioorg Med Chem Lett 18*, 6501-6504.

Figure legends

Figure 1 Structures of receptor tyrosine kinase inhibitors used in this study. [**1**] Crizotinib; [**2**] TAE684; [**3**], PD0325901; [**4**] Vatalanib; [**5**] PDGFR/Kit tyrosine kinase inhibitor IV.

Figure 2 NPM-ALK and NPM-Ltk expression drives iridophore development. **a**) Schematic of experiment. Note that the *sox10* promoter fragment used in this construct has been shown to drive expression in neural crest (*20*), so that these transiently transgenic embryos are expected to express the activated ALK or Ltk kinase in a tissue-specific, but mosaic, manner. **b-e**) Injection of 230 pg of p*sox10:NPM-ALK* into wild-type (**c**) or ltk^{ty82} mutants (**e**) increases iridophore numbers compared with uninjected controls (**b,d**). Iridophores are the prominent silver-gold spots, seen either as individual cells (yellow arrowheads in **b**), or as clusters (e.g. on surface of eye (e) in **b**). In wild-types, expression generates supernumerary (arrows) and ectopic (arrowheads) iridophores, whereas in *ltk* mutants iridophore development is rescued, often forming large clusters (arrows). **f-i**) Analogous experiment using p*sox10:NPM-Ltk* gave very similar phenotypes. All fish photographed at 5 dpf. NB Fish in panels **b-e** have been treated with phenylthiourea and hence lack melanin. Here and in all subsequent figures, embryos are shown dorsal up, and anterior to left. Scale bar, 200 µm.

Figure 3 TAE684 inhibits NPM-ALK *in vivo* and reduces endogenous iridophores. Wild-type embryos were injected with 50 pg of p*sox10:NPM-ALK* and treated with 2 µM of TAE684 ALK inhibitor or DMSO control. **a**) Schematic of experiment in **Figure 3** and **Figure 4**. **b-d**) Incident light images at 3 dpf of control uninjected, non-treated embryo (**b**), NPM-ALK injected DMSO-treated sibling (**c**) and NPM-ALK injected TAE684-treated siblings (**d**). Injected embryos (**c**) have ectopic (arrowheads) and supernumerary (arrows) iridophores when compared to the uninjected control (**b**). Injected embryo treated with TAE684 has fewer iridophores than controls in eyes and trunk (asterisks) and no ectopic iridophores or large clusters (**d**). Ratios of embryos with normal, ectopic/supernumerary and decreased iridophore numbers are quantitated in **e**). Differences between treatments are significant (Freeman-Halton extension of Fisher exact probability test, *p* values shown); numbers treated (n) in each category shown below each column. **f**) Iridophore number in dorsal stripe position after treatment with Crizotinib and/or MEK inihibitor PD0325901 (PD0325). Comparisons assessed using Fisher's exact probability test. Note that Crizotinib treatment results in significant decrease in ectopic/supernumerary iridophore number compared with controls, and that a low dose (500 nM) of PD0325901 (ineffective on its own) sensitises for the Crizotinib effect. Scale bar, 200 µm.

Figure 4 TAE684 inhibits NPM-Ltk. Wild-type embryos were injected with 30 pg of p*sox10:NPM-Ltk* and treated with 3 µM of TAE684 (for schematic see **Figure 3**). Incident light images (**a-c**) at 3 dpf of control uninjected, non-treated embryo (**a**), NPM-Ltk injected, DMSO-treated sibling (**b**) and NPM-Ltk injected TAE684-treated siblings (**c**). Injected embryos (**b**) have ectopic (arrowheads) and supernumerary iridophores (arrows) when compared to the uninjected control (**a**). Injected, TAE684-treated embryos have fewer iridophores than control in eyes and trunk and no ectopic iridophores or large clusters (**c**). Ratios of embryos with different phenotypes are

quantitated in **d**), as in **Figure 3e**); differences between treatments are significant (Freeman-Halton extension of Fisher exact probability test, *p* values shown). Scale bar, 500 µm.

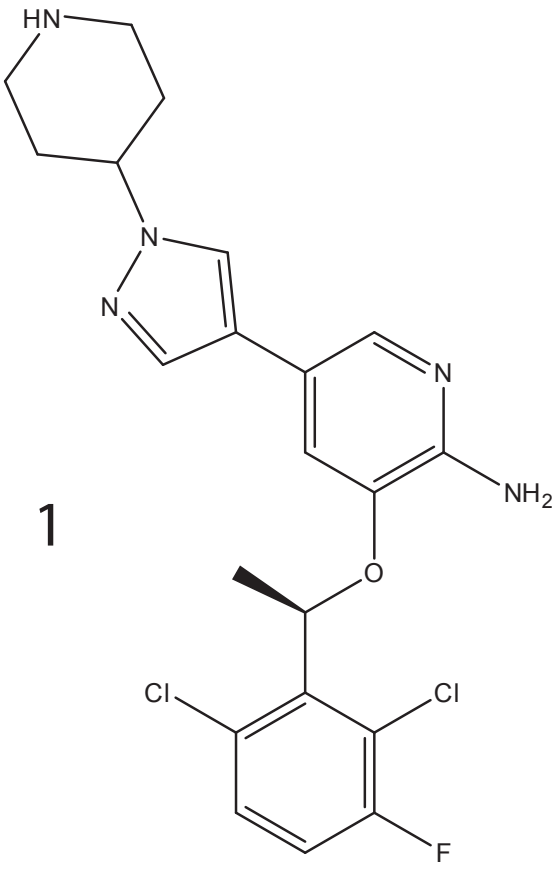
HN
N
N
N
NH2
O
Cl
Cl
F

1

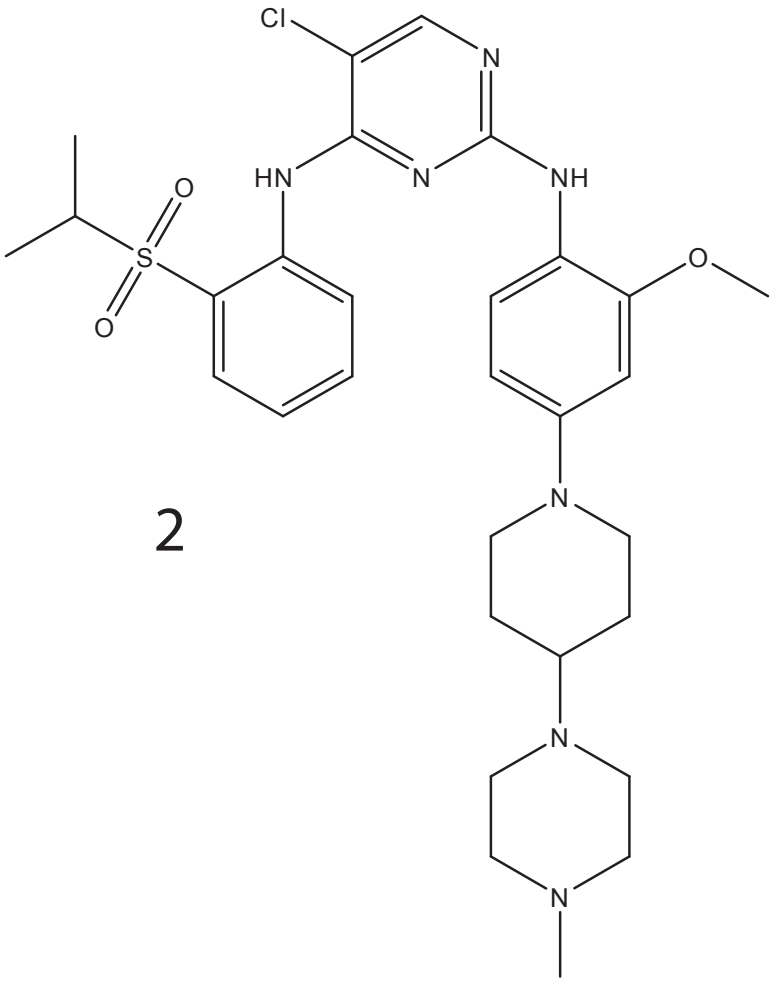
Cl
N
HN
N
NH
O
S
O
O
N
N
N
N

2

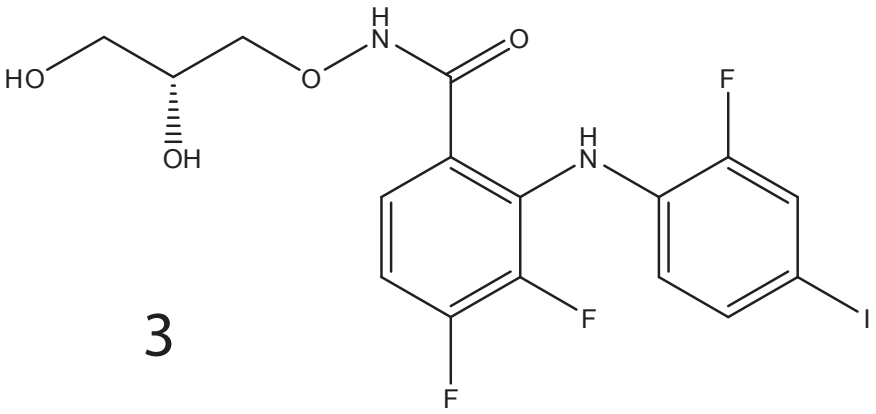
HO
OH
O
H
N
O
H
N
F
F
F
I

3

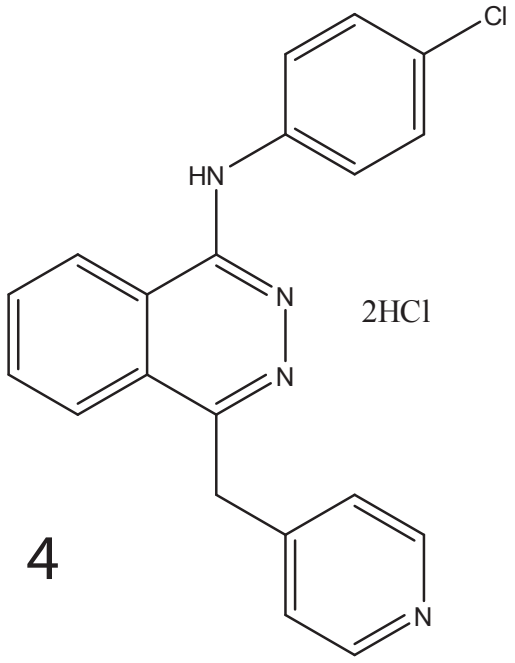
Cl
HN
N
N
2HCl
N

4

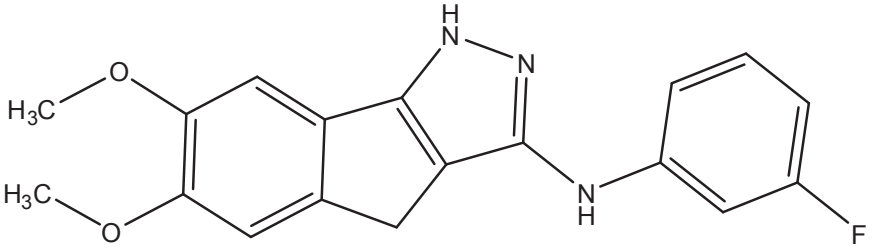
H
N
N
O
H3C
H3C
O
N
H
F

5

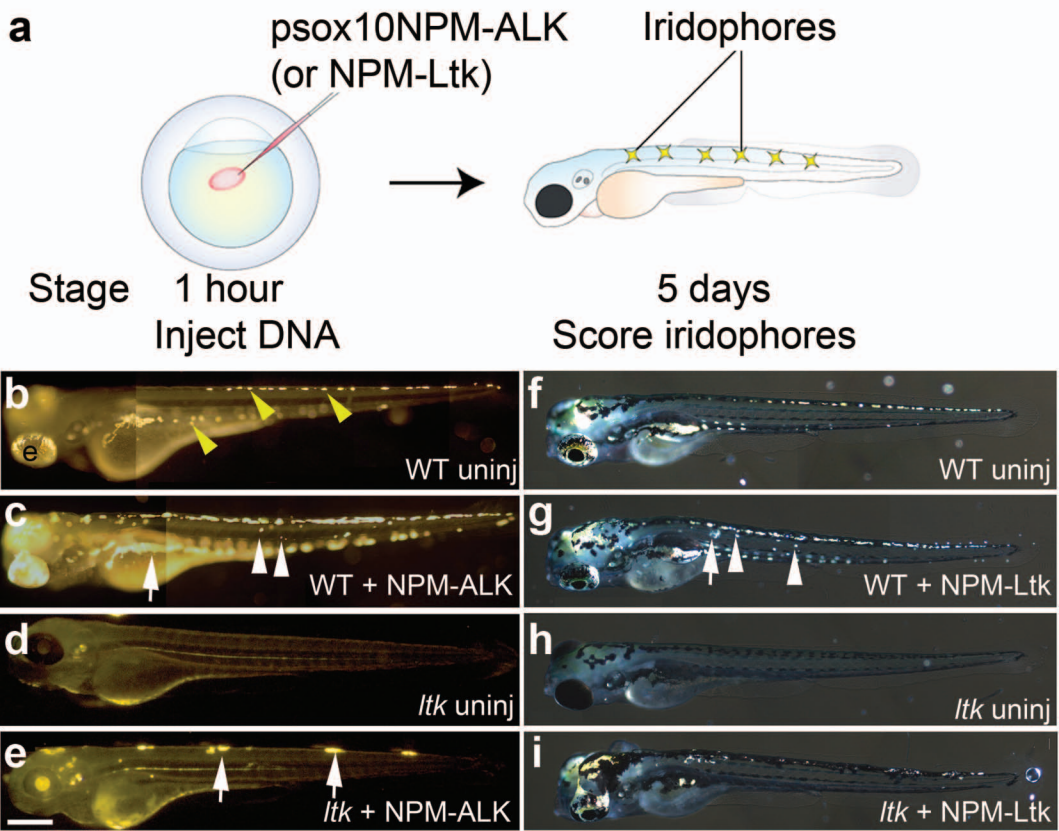
a
psox10NPM-ALK
(or NPM-Ltk)
Iridophores
Stage
1 hour
Inject DNA
5 days
Score iridophores
b
WT uninj
c
WT + NPM-ALK
d
ltk uninj
e
ltk + NPM-ALK
f
WT uninj
g
WT + NPM-Ltk
h
ltk uninj
i
ltk + NPM-Ltk

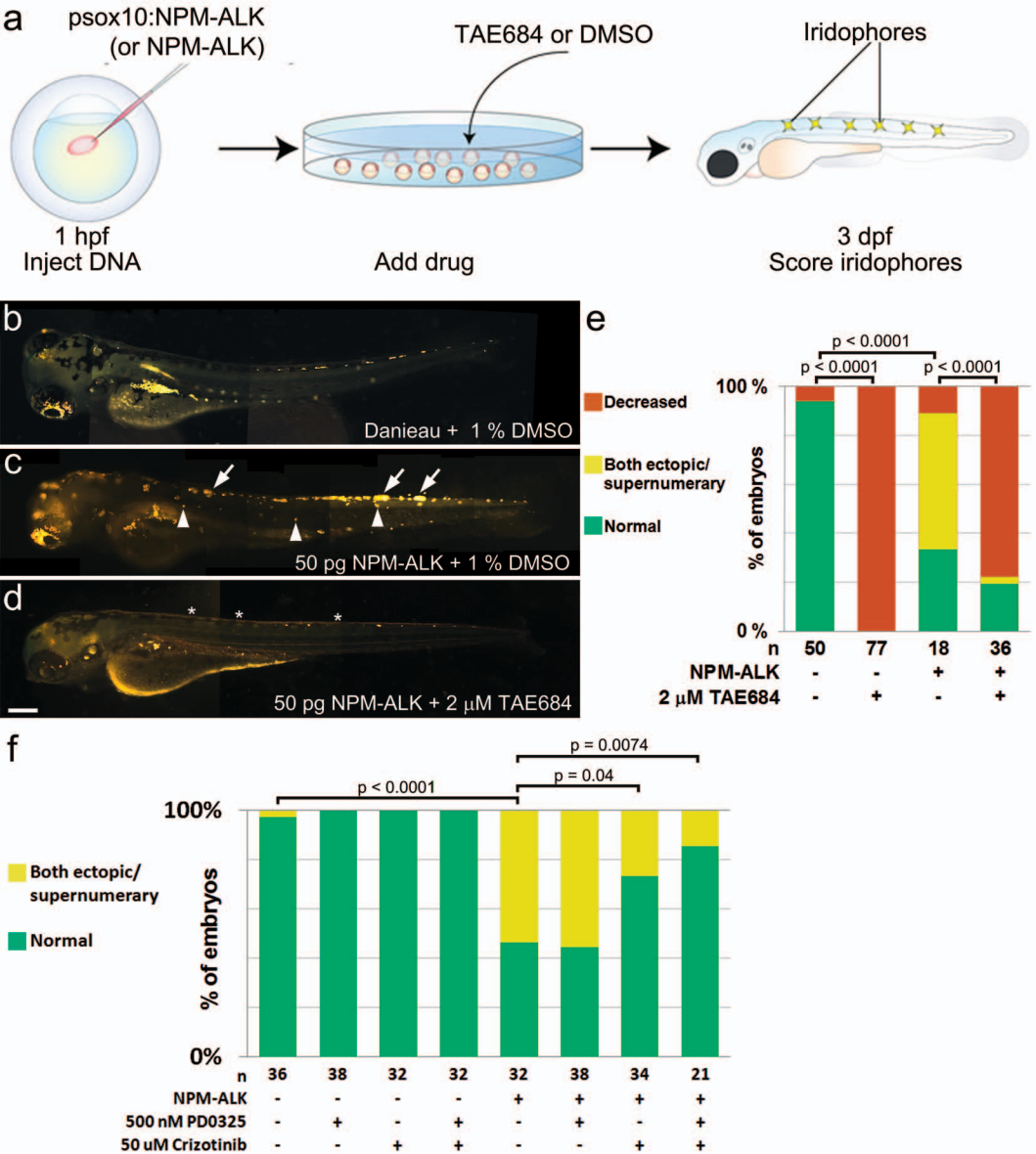
a
psox10:NPM-ALK
(or NPM-ALK)
TAE684 or DMSO
Iridophores
1 hpf
Inject DNA
Add drug
3 dpf
Score iridophores
b
Danieau + 1 % DMSO
c
50 pg NPM-ALK + 1 % DMSO
d
50 pg NPM-ALK + 2 μM TAE684
e
p < 0.0001
p < 0.0001
p < 0.0001
Decreased
Both ectopic/
supernumerary
Normal
100 %
0 %
% of embryos
n 50 77 18 36
NPM-ALK - - + +
2 μM TAE684 - + - +
f
p = 0.0074
p = 0.04
p < 0.0001
100%
0%
Both ectopic/
supernumerary
Normal
% of embryos
n 36 38 32 32 32 38 34 21
NPM-ALK - - - - + + + +
500 nM PD0325 - + - + - + - +
50 uM Crizotinib - - + + - - + +

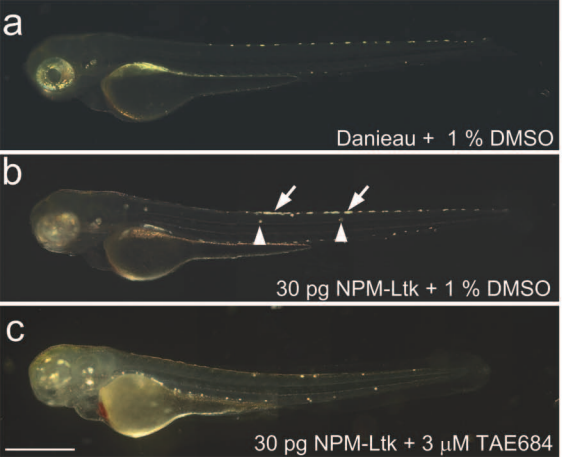
a
Danieau + 1 % DMSO
b
30 pg NPM-Ltk + 1 % DMSO
c
30 pg NPM-Ltk + 3 μM TAE684
d
p < 0.0001
p < 0.0001
p < 0.0001
Decreased
Both ectopic/
supernumerary
Normal
100 %
0 %
% of embryos
n 66 55 75 82
NPM-Ltk - - + +
3 μM TAE684 - + - +